

SAGD Reservoir Characterization Using Geostatistics: Application to the Athabasca Oil Sands, Alberta, Canada

Jason A. McLennan and Clayton V. Deutsch

Department of Civil & Environmental Engineering
University of Alberta

Abstract

The application of Steam Assisted Gravity Drainage (SAGD) is important because of the vast reserves accessible with this production mechanism. The Athabasca Oils Sands, also known as the McMurray Formation, is located in northern Alberta near Fort McMurray. The McMurray Formation contains an estimated one-trillion barrels of bitumen-in-place or one-quarter of Canada's total oil reserves; however, only 10% is economically recoverable by surface mining techniques currently being used. An estimated additional 25% of the Athabasca Oil Sands is economically recoverable using SAGD extraction.

SAGD production performance is the oil production rate OP_{RATE} and the cumulative steam-to-oil ratio SOR . These production variables depend on geological heterogeneity, which is essentially the distribution of petrophysical properties within the distribution of facies. However, in between well locations, the geological heterogeneity is impossible to exactly predict and there is unavoidable geological uncertainty. This geological uncertainty can be transferred to production performance uncertainty using geostatistics. Geostatistical simulation provides multiple geological realizations, which combine to form a quantitative model of geological uncertainty.

Several post-processing steps are performed on the geological realizations to characterize the reservoir for SAGD extraction processes. These include (1) calculate "local connectivity" and perform a "connected resource assessment", (2) determine the drainage volume of a potential SAGD well pair, (3) extract the geological realizations within the drainage volume, (4) down-scale the geological realizations within the drainage volume, (5) rank the fine-scale geological realizations and select low, medium and high cases for flow simulation input, (6) perform flow simulation for OP_{RATE} and SOR and (7) calibrate the OP_{RATE} and SOR results to the geological ranking parameter.

Introduction

About 100 million years ago, streams from the western Rocky Mountains and the eastern Precambrian Shield drained into the northern portion of the Canadian Prairie Province of Alberta forming a massive inland sea. The erosion and suspension of sandstones and mudstones upstream were deposited relatively flat during subsequent fluvial, estuarine and marine phases of the sea. After dehydrating, the sea sediments were capped by marine shale, which is currently referred to as the Clearwater Formation. Oil then percolated into the high porosity sediment pores. Although there is debate, popular opinion among geologists suggests that the oil came from somewhere else, specifically, from highly organic cretaceous shale in the southern portion of the Alberta Sedimentary Basin.

The Athabasca Oil Sands, also known as the McMurray Formation, is located 50km northwest of Fort McMurray, Alberta. The McMurray Formation spans 40,000 km² and contains an estimated one-trillion barrels of bitumen-in-place. This amount is 70% of Alberta's total oil reserves and 25% of Canada's. Syncrude Canada Ltd. and Suncor Energy Inc. currently apply surface mining

extraction techniques in the McMurray Formation to produce an equivalent 22% of Canada's total annual oil production. However, only 10% of the Athabasca Oil Sands is located close enough to the surface to allow for economical surface mining extraction methods. The demand for innovative in-situ oil sands extraction technology to recover deeper oil sands is high.

SAGD is a thermal in-situ heavy oil recovery process. Essentially, steam is injected into an injection well forming a cone-shaped steam chamber. As the steam chamber expands, new bitumen is heated and replaced by steam; the heated bitumen lowers in viscosity and flows downward along the steam chamber boundary into a production well by way of gravity. The SAGD process was pioneered in 1978 by Dr. Roger Butler, holder of the Endowed Chair of Petroleum Engineering at the University of Calgary from 1983 to 1995. By 1997, the underground test facility (UTF) project successfully demonstrated the commercial viability of SAGD extraction technology in the Athabasca Oil Sands.

The primary SAGD production performance parameters are the rate oil is produced out of the production well and the cumulative amount of steam needed to propel the steam chamber to produce the target production rate. The latter is referred to as OP_{RATE} while the former is referred to as SOR. High OP_{RATE} and low SOR variable values are desirable.

Reservoir geology affects SAGD production performance. Consider, for example, the two identical SAGD well pair configurations in Figure 1. One well pair is located directly below a large vertically extensive volume of sand and the other is located directly below an aerially extensive shale lens. The OP_{RATE} and SOR performance of the well pair located below the sand facies will be significantly better (higher OP_{RATE} and lower SOR) than the well pair located below the shale lens. This is because the steam chamber is not blocked by an overlying shale lens. Lithology, especially the distribution of impermeable shale, affects SAGD production performance. In addition to lithology, other spatially dependant geological parameters such as thickness, porosity, permeability, oil saturation, gas saturation and water saturation, affect OP_{RATE} and SOR.

Exploration wells and coreholes can be used to help delineate the geological properties of a reservoir. However, geological heterogeneity is impossible to exactly predict between wells and/or coreholes. The unique true distribution of lithofacies and petrophysical properties is and will remain unknown. Geological uncertainty, therefore, is an inherent characteristic of any geological model. Therefore, since geology affects SAGD production performance, OP_{RATE} and SOR are also inherently uncertain.

Geostatistics can be used to quantify geological uncertainty. Geostatistical simulation allows for the construction of multiple realizations that can be combined into a histogram of uncertainty. Although there are other sources of uncertainty such as scaling processes, fluid property measurements, numerical approximations in flow simulation and so on, the uncertainty captured by geostatistical structure, facies, porosity and permeability models are the most significant. Geological uncertainty is then quantified by simulating multiple structure, lithology, porosity and permeability realizations.

The main purpose of characterizing a SAGD reservoir using geostatistics is to quantify OP_{RATE} and SOR production performance uncertainty based on geological (lithology, porosity and permeability) uncertainty. The uncertainty in OP_{RATE} and SOR production performance variables are linked to the geological uncertainty through flow simulation and a geological ranking parameter. These two links are important.

Flow simulation is CPU-expensive due to the relatively complex geological heterogeneities and numerical thermal modeling. For this reason, relatively few flow simulations can be performed. That is, it is neither possible nor necessary to process all the geostatistical realizations through the

flow simulator. Selected *low* (p10), *medium* (p50) and *high* (p90) geological realizations are flow simulated. This selection permits the inference of flow response for the other geological realizations at the same location. The calibration of flow response to geological heterogeneity through a geological ranking parameter allows the prediction of flow response at locations where no flow simulation was performed. Of course, it is not possible to exactly predict the flow behavior; however, we can quantify the uncertainty associated with this extrapolation.

The uncertainty in SAGD production performance can be used to determine the number and location of SAGD well pairs required to achieve a specified production target. Within physical constraints of SAGD well placement, areas of high OP_{RATE} and SOR production potential can be drilled first. Additional exploratory wells and/or coreholes would reduce production performance uncertainty and permit more accurate well planning. For example, fewer well pairs, in more optimal locations, would need to be drilled for the same production target.

This paper outlines the methodology for SAGD reservoir characterization using geostatistics within the Athabasca Oil Sands. The main steps for geostatistical modeling are (1) simulate multiple realizations of the reservoir structure (top and bottom surface), (2) simulate multiple lithofacies realizations within the reservoir structure and (3) simulate multiple petrophysical property realizations within the lithofacies and structure models.

Additional post-processing steps towards characterizing the reservoir specifically for a SAGD extraction process then need to be taken. These include (1) calculate local connectivity and perform a connected resource assessment, (2) determine the drainage volume of potential SAGD well pairs, (3) extract the geological realizations within the drainage volumes, (4) down-scale the geological realizations within the drainage volumes, (5) rank the fine-scale geological realizations and select low, medium and high cases for flow simulation input, (6) perform flow simulation for OP_{RATE} and SOR and (7) calibrate the OP_{RATE} and SOR results to the geological ranking parameter.

Methodology

A first step in the SAGD reservoir characterization process is to explore some basic statistical characteristics of the geological variables. Histograms and scatter plots of the model variables facilitate understanding of reservoir geology and stationarity. Geostatistical simulation requires representative statistics.

The large scale reservoir structure must be established. The reservoir volume is defined by the top and bottom surfaces and thickness. The Top McMurray T_{MCM} and Bottom McMurray B_{MCM} surfaces define the limits of the Athabasca Oil Sands. Thickness *Thick* is simply $T_{MCM} - B_{MCM}$. SAGD production performance depends on the reservoir volume; therefore, structural uncertainty must be quantified and eventually transferred to SAGD production uncertainty. To quantify structural uncertainty, multiple geostatistical realizations of the T_{MCM} , B_{MCM} and *Thick* variables are created conditioned by all available elevation data:

$$\begin{aligned} T_{MCM}^{(l)}(\mathbf{u}_h), \quad h = 1, \dots, H, l = 1, \dots, L \\ B_{MCM}^{(l)}(\mathbf{u}_h), \quad h = 1, \dots, H, l = 1, \dots, L \\ Thick(\mathbf{u}_h) = T_{MCM}^{(l)}(\mathbf{u}_h) - B_{MCM}^{(l)}(\mathbf{u}_h), \quad h = 1, \dots, H, l = 1, \dots, L \end{aligned} \quad (1)$$

The locations \mathbf{u}_h , $h = 1, \dots, H$ represent the aerial grid cell locations. The number of realizations $l = 1, \dots, L$ should be sufficient to reflect uncertainty and avoid decision making based on unrepresentative stochastic features (20-100 are considered sufficient).

An appropriate grid system for modeling lithofacies and petrophysical properties must be established within the reservoir volume. The basic topology used in most geostatistical reservoir modeling is Cartesian, defined by cell-centered aerial grids and isochore vertical grids. These grid systems are compatible with subsequent scaling and flow simulation operations. The number of cells (resolution) is a balance between the benefit of heterogeneous detail and the cost of computer resources.

Reservoirs are made up of a sequence of genetically related strata or layers. The existing structure and original structure of the reservoir is almost always different due to various structural deformation processes. The goal is to implement geostatistical calculations such as variography within each layer's original (natural) geological structure while preserving the existing reservoir structure in the final model. A stratigraphic vertical coordinate that restores the layer's existing structure to its original structure must be considered for directional geostatistics calculations.

The uncertainty in lithofacies must be quantified and transferred to SAGD production uncertainty. There are a variety of facies modeling techniques available, broadly grouped into object-based modeling and cell-based modeling. Indicator simulation is a cell-based technique that has proven applicable when it is not possible to infer simple clean shapes for object-based modeling. The steps for cell-based geostatistical facies modeling include (1) identify and code the facies to be modeled, $f = 1, \dots, F$, where f is the integer code of F lithofacies to be modeled, (2) construct the target facies distribution, which is the proportion of each of the F facies, (3) investigate 3-D trends within each of the F facies and (4) assemble a licit 3-D variogram model within each of the F facies types. Multiple geostatistical lithofacies realizations are created conditional to the raw facies data from exploration wells/coreholes, global facies proportions, 3-D proportion trends and 3-D variograms:

$$Fcs^{(l)}(\mathbf{u}_n), \quad n = 1, \dots, N, l = 1, \dots, L \quad (2)$$

The locations \mathbf{u}_n , $n = 1, \dots, N$ represent the 3-D grid cell locations. Each facies realization is clipped by one structure realization. For example, the $F^{(l)}(\mathbf{u}_n)$ values above $T_{MCM}^{(l)}(\mathbf{u}_n)$ or below $B_{MCM}^{(l)}(\mathbf{u}_n)$ are outside the reservoir volume and clipped.

The uncertainty in porosity and permeability must be quantified and transferred to SAGD production uncertainty. These petrophysical properties are significantly controlled by the lithofacies they are contained in; therefore, porosity and permeability are modeled separately within each of the F facies. The basic steps include (1) construct the target distribution within each of the F facies, (2) investigate trends within each of the F facies and (3) build a 3-D variogram model within each of the F facies. Additional attention is required for scaling and averaging operations performed on the permeability variable. Multiple porosity and permeability realizations are created conditional to the raw well/corehole data, the target distributions, the 3-D trend models and the 3-D variogram models:

$$\begin{aligned} \phi^{(l)}(\mathbf{u}_n), \quad n = 1, \dots, N, l = 1, \dots, L \\ k^{(l)}(\mathbf{u}_n), \quad n = 1, \dots, N, l = 1, \dots, L \end{aligned} \quad (3)$$

where ϕ and k represent porosity and permeability, respectively. Each porosity and permeability model is merged into one facies realization using a "cookie cutter" approach. That is, the porosity and permeability variables are first simulated assuming the entire structure is one facies type for as many facies types exist then mapped into the final porosity and permeability models using the facies realizations. For example, for the $Fcs^{(l)}(\mathbf{u}_N)$ value, the final $\phi^{(l)}(\mathbf{u}_N)$ and $k^{(l)}(\mathbf{u}_N)$ values are equal to the simulated porosity and permeability at \mathbf{u}_N assuming the entire model space is equal to

the $F^{(l)}(\mathbf{u}_N)$ facies type. Other petrophysical properties such as oil, gas and water saturation may also be modeled using a similar procedure.

One geological realization contains one structure, one lithofacies and one petrophysical property realization. The variation between the L geological realizations defines the reservoir's geological uncertainty. Based on this geological variation, the goal is to define the variation in production performance parameters, OP_{RATE} and SOR . The suite of L geological realizations is then used to characterize the reservoir specifically for a SAGD thermal extraction process.

Before using the geological realizations to characterize the reservoir for SAGD potential, it will help to define a net grid cell indicator based on the geology. A possible transform criterion is:

$$i_{net}^{(l)}(\mathbf{u}_n) = \begin{cases} 1, & \text{if } Fcs^{(l)}(\mathbf{u}_n) \neq \text{shale}, \phi^{(l)}(\mathbf{u}_n) > \phi_t, k^{(l)}(\mathbf{u}_n) > k_t \\ 0, & \text{otherwise} \end{cases} \quad n = 1, \dots, N, l = 1, \dots, L \quad (4)$$

where $Fcs^{(l)}(\mathbf{u}_n)$ is the facies value, $\phi^{(l)}(\mathbf{u}_n)$ is the porosity value, ϕ_t is a porosity threshold, $k^{(l)}(\mathbf{u}_n)$ is the permeability value and k_t is a permeability threshold.

SAGD reservoir characterization should involve a local connectivity calculation. Local connectivity is defined as either the success or failure of the steam chamber to reach and recover bitumen within an expected SAGD drainage volume. Consider the three well pairs and their associated drainage areas in Figure 2. The drainage areas are superimposed on a cross section that indicates net reservoir areas. A conventional connectivity calculation would determine only whether or not the entire net reservoir is connected. This is problematic because a steam chamber is not expected to reach and recover the oil outside the limits of its expected drainage volume; only oil within an expected drainage volume could possibly be recovered. Therefore, local connectivity, that is, connectivity inside the expected steam chamber drainage volumes, must be assessed.

A program that calculates local connectivity is developed. The local connectivity program takes on the form of an indicator transform:

$$i_{conn}^{(l)}(\mathbf{u}_n) = \begin{cases} 1, & \text{if connected} \\ 0, & \text{if unconnected} \end{cases} \quad n = 1, \dots, N, l = 1, \dots, L \quad (5)$$

Figure 2 illustrates the general results of the local connectivity calculation within the three SAGD well pairs shown. A grid cell that is deemed connected must itself have $i_{net}^{(l)}(\mathbf{u}_n) = 1$ and be adjacent to $i_{net}^{(l)}(\mathbf{u}_n) = 1$ cells inside the drainage volume that, together, form a path for oil to drain into the SAGD production well.

Connectivity is calculated within windows centered on each column of grid cells in the reservoir. The width of these calculation windows is input to represent the expected drainage volume width typical of SAGD well pairs in the reservoir. The geological model is input, with net lithology and porosity and permeability net threshold specifications, to define the $i_{net}^{(l)}(\mathbf{u}_n)$ indicator, which is the net reservoir. Connectivity of a particular column is calculated for only those grid cells in the same column, although they may be connected through cells belonging to other columns the width of the calculation window. There are usually multiple connected columns within one column of grid cells, in which cases, only the lowest-thickest connected column is considered connected. The base elevations of the connected reservoir are, therefore, the elevations of the lowest elevation cell in the lowest-thickest column of connected cells. Other than the connectivity indicator and the connected bottom output, a number of other useful outputs are available from the local connectivity program. These include the facies type of the connected cells and the number of adjacent connected cells in 3-D, the connected column thicknesses and the ratio of

connected column thicknesses to structure thicknesses in 2-D, and the global proportion of connected to unconnected reservoir cells.

The language of probability is a well-established way to express uncertainty. Local connectivity uncertainty can be quantified based on geological uncertainty. Perhaps the best summary of local connectivity and its uncertainty is the probability of connection:

$$P_{conn}(\mathbf{u}_n) = \frac{\sum_{l=1}^L i_n^{(l)}}{L} \quad n = 1, \dots, N \quad (6)$$

A connected resource assessment is performed to indicate the potential recoverable reserves using a SAGD extraction process. The geological realizations or uncertainty can be used to calculate the uncertainty in SAGD recoverable reserves. The main parameter of interest is the connected contained bitumen:

$$Q^{(l)} = \sum_{n=1}^N V(\mathbf{u}_n) \cdot \phi^{(l)}(\mathbf{u}_n) \cdot (1 - S(\mathbf{u}_n)) \cdot i_{net}^{(l)}(\mathbf{u}_n) \cdot i_{conn}^{(l)}(\mathbf{u}_n) \quad l = 1, \dots, L \quad (7)$$

where $Q^{(l)}$ is the connected contained bitumen, $V(\mathbf{u}_n)$ is the grid cell volume, $\phi^{(l)}(\mathbf{u}_n)$ is the porosity value, $S(\mathbf{u}_n)$ is the water saturation value, $i_{net}^{(l)}(\mathbf{u}_n)$ is the net cell indicator in (4) and $i_{conn}^{(l)}(\mathbf{u}_n)$ is the connectivity indicator in (5). Note, a grid cell's contained bitumen is only included in the summation if it is not shale, it is above a specified porosity and permeability threshold and it is connected. An important assumption in this calculation is that the entire reservoir is produced by non-overlapping steam chamber drainage volumes. Other SAGD resource assessment parameters such as the volume of shale, connected sand thickness, average net porosity, average net permeability, and so on could also be calculated.

Subsequent steps of the SAGD reservoir characterization process deal with preparing the input for flow simulation, which will provide SAGD performance parameters, namely OP_{RATE} and SOR .

The geological realizations within nDV potential SAGD drainage volumes are extracted from the reservoir. The result is L sets of structure (top and bottom surface), lithofacies and petrophysical property realizations within nDV potential SAGD drainage volumes. The idea is to extract nominal steam chamber volumes of influence for potential SAGD well pairs. In addition, the local connectivity window size and the required detail and available computer resources to run flow simulation influence the drainage volume dimensions.

Flow simulation is usually performed to capture large scale flow interactions based on an up-scaled (coarse) version of the reservoir geology; however, flow simulation for SAGD performance computation is an exception because OP_{RATE} and SOR are affected by the steam chamber and oil flow interactions within a subset of the reservoir approximately equal to the nominal SAGD drainage volumes. For each of the nDV extracted drainage volumes, therefore, the L geological realizations are down-scaled into a finer resolution geological model appropriate for calculating SAGD flow response. Various techniques are available to scale coarse resolutions down to finer resolutions, such as mathematical scaling relationships or interpolation algorithms. Another possibility is re-simulating the extracted SAGD drainage volumes to a finer grid using the extracted geological realizations for conditioning data.

Not all L fine scale geological realization within all nDV SAGD drainage volumes can be input into the flow simulator due to the high computer resources demand. A geological ranking parameter that is well correlated to OP_{RATE} and SOR such as sand volume, shale volume or net connected volume can be calculated for all L fine scale geological realizations within all nDV

drainage volumes. Low (p10), medium (p50) and high (p90) ranking parameter realizations span the geological uncertainty and, since OP_{RATE} and SOR is well correlated to the ranking parameter, would sufficiently span SAGD production performance uncertainty. To reduce computer resources demand, these selected cases are input into flow simulation. In practice multiple, drainage volume locations exist. To further reduce flow simulation input, the drainage volume locations can be ranked according to the expected geological ranking parameter value and a similar ranking and selection procedure can be performed

Flow simulation provides OP_{RATE} and SOR for every selected drainage volume realization; these results must be calibrated. Figure 3 shows the OP_{RATE} and SOR flow results versus the sand volume ranking parameter for twelve drainage volume selections – low, medium and high sand volume realizations from low, medium-low, medium-high and high sand volume locations – within a real potential SAGD reservoir in the McMurray Formation. Based on the correlation developed in these twelve cases, a synthetic flow response is developed for any possible drainage volume location with any particular sand volume. The geological uncertainty, which is the variation in the L geologic realizations, can be transferred to uncertainty in SAGD well pair production performance uncertainty given the link in Figure 3. Figure 4 shows the uncertainty in cumulative OP_{RATE} versus the number of well pairs. This uncertainty could be reduced by drilling additional exploratory wells or coreholes. It is possible to identify and order areas with the greatest geologic potential. The ordering could be based on the geological ranking system since it is highly correlated with SAGD productivity.

An application to the Athabasca Oil Sands illustrates the necessary steps to prepare a single potential SAGD drainage volume for flow simulation.

Application

The data used in this example are a subset of coreholes extracted from a real dataset within the McMurray Formation. Twenty exploration coreholes are positioned onto a 400 x 400m grid, see Figure 5. There are 4 coreholes in the easting direction and 5 coreholes in the northing direction spanning an area 1600m east-west by 2000m north-south. The coreholes are exactly vertical. Six variable values are available at 10cm vertical increments down each corehole: Nch – the corehole number, X – the easting coordinate (m), Y – the northing coordinate (m), Z – the elevation coordinate (meters above sea level – masl), Fcs – the facies type (integer code), and Por – the porosity (%). These six variable values are illustrated for corehole 9 ($Nch = 9$) in Figure 5.

Porosity is the only petrophysical property modeled here; nevertheless, the SAGD reservoir characterization process is the same when, in practice, other petrophysical properties such as permeability, oil saturation and gas saturation may have to be modeled.

A histogram of the facies Fcs and porosity Por variable are shown in Figure 6. Declustering is not performed because the coreholes are uniformly spaced. The proportions of sand, interbedded sand, shale and breccia are 51%, 22%, 18% and 9%, respectively. The mean and variance of the porosity variable are 21% and 2%, respectively. The shape of the porosity distribution is tri-modal where each mode represents a facies-controlled porosity population. The mean porosity in sand, interbedded sand, shale and breccia is 32%, 15%, 1% and 20%, respectively. Subsequent facies and porosity modeling must reproduce the distributions in Figure 6. Sand, interbedded sand and breccia are net facies – shale is a non-net facies.

The structure of the reservoir is modeled using a geostatistical procedure, see Figure 7. There are 20 top and 20 bottom elevation conditioning data. The top elevations are located in the first reliable net facies presence and the bottom elevations are located in the first reliable non-net facies. Experimental top and bottom surface elevation variograms are calculated and modeled

using a single Gaussian structure of isotropic range and 0 nugget. 100 geostatistical realizations of the top and bottom surface elevations are then simulated using a 50 x 50m aerial block size. The 50th top and bottom surface realizations are superimposed on the corresponding top and bottom conditioning data in Figure 7.

The Athabasca Oil Sands were deposited relatively flat. The top and bottom surfaces are not exactly flat, however, due to sand accumulation at the top and space filling at the bottom, respectively. Minimal structural deformation has taken place since the time of deposition. The 3-D expected (cell average) top and bottom surfaces are shown in Figure 8. A central cross section through the grid in each direction is also shown in a projected view. The grid is a cell-centered Cartesian system. The vertical dimension of the cells is 0.5m. The stratigraphic coordinate system used is vertical and measured in masl. This simple vertical coordinate system is consistent with the flat correlation styles characteristic of the McMurray Formation and will account for channel filling and accumulation.

Indicator simulation is used to construct a cell-based facies Fcs variable model. Facies trends are significant and are considered. For each facies type, a 1-D vertical proportion curve is calculated and a 2-D horizontal proportion map is estimated using a smooth kriging scheme. These are combined into a 3-D facies proportion model and used to condition the facies simulation. The spatial model of correlation of each of the facies will also condition the simulation. Vertical and horizontal facies variograms are calculated and combined into 3-D variogram models within each facies. 100 geostatistical realizations of the facies Fcs variable are constructed using the raw corehole data, the facies trend models and the facies variogram models for conditioning information. Each facies realization is clipped by the top and bottom surface of one structure realization. Easting, northing and two elevation cross sections through the 50th facies realization are shown in Figure 9 with the raw facies corehole data.

A sequential Gaussian simulation algorithm is implemented to model the porosity Por variable within each net facies. A 3-D porosity trend is constructed by combining a 1-D vertical mean porosity curve with a 2-D horizontal porosity map estimated using a smooth kriging scheme within each net facies type. Vertical and horizontal porosity variograms are calculated and combined into 3-D models within each net facies. Three sets of 100 porosity simulations are performed. Each set is simulated assuming one net facies is 100% present throughout the model space and using the corresponding net facies raw corehole data, trend model and variogram model as conditioning information. The facies realizations are used to map the porosity values into the appropriate facies locations. If the facies is non-net (shale), the porosity is set to 0%. One facies realization is used to map one porosity realization. Easting, northing and two elevation cross section through the 50th porosity realization are shown in Figure 10 with the raw porosity corehole data.

The connectivity of each geological realization is calculated by implementing the local connectivity algorithm previously described. Each grid cell is coded according to (4). A column width of 150m (3 cells) is used. Net facies cells are defined as being (1) above a 9% porosity threshold and (2) in either sand, interbedded sand or breccia lithology. Shale is input as a non-net facies. Over all 100 realizations, the average proportion of cells that are connected is 85% per realization (206,720 cells out of 243,200 cells). The 50th connectivity realization is shown in Figure 11; the probability of each cell being connected is also calculated and shown. Comparing Figure 11 to the facies model in Figure 9 indicates the significant influence non-net shale facies has on local connectivity.

The connected contained bitumen is calculated for each geological realization. Net facies are now defined as being (1) connected, (2) above a 9% porosity threshold and (3) in either sand, interbedded sand or breccia lithology. The volume of each cell is 1250m³ (50 x 50 x 0.5m) and

water saturation is assumed constant at 15%. Figure 12 shows the results in a histogram and probability plot. The p10, p50 and p90 connected contained bitumen values are 28.8, 29.6 and 30.4 in units of million m³.

Figure 13 shows the location of the volume chosen to prepare for flow simulation. The volume dimensions are 1000 x 150 x 190m in the easting, northing and elevation directions, respectively. This subset of the reservoir is assumed to be the cumulative steam chamber drainage volume anchored by a horizontal injection well 25m above the bottom surface. Within this drainage volume, the suite of geological realizations are extracted and used as conditioning data to simulate fine-scale versions of the geological realizations. The down-scaling procedure increases the resolution of the geological model within the drainage volume by factors of 5, 50 and 1 in the easting, northing and elevation directions, respectively. The 50th high resolution facies and porosity realization is shown in Figure 13. These high resolution geological drainage volume models are now appropriate for OP_{RATE} and SOR production performance calculations using flow simulation; however, not all 100 realizations can be practically run through the flow simulator.

The 100 fine-scale geological drainage volume realizations are ranked according to connected drainage volume. For each fine-scale geological drainage volume realization, connected drainage volume is the sum of the 5m³ (10 x 1 x 0.5m) cell volumes that are and are next to a net facies, where net facies is defined as being above 9% porosity and in either sand, interbedded sand or breccia lithology. The histogram and probability plot of the results are shown in Figure 14. Each realization is a connected drainage volume percentile. The p10, p50 and p90 connected drainage volume percentiles in units of million m³ are 8.65, 9.09 and 9.58 and correspond to the 49th, 68th and 3rd geological realizations, respectively. These three geological drainage volume realizations can be input into flow simulation for the calculation of OP_{RATE} and SOR parameters that sufficiently span SAGD production performance within the selected drainage volume. This is due to excellent correlation between SAGD production performance and connected drainage volume. And this correlation relationship is the link to OP_{RATE} and SOR uncertainty from geological uncertainty.

Discussion

There are two main aspects to predicting SAGD production uncertainty: (1) characterizing geological uncertainty and (2) transferring geological uncertainty into production uncertainty. Geological uncertainty is characterized by simulating multiple structure, lithofacies and petrophysical property realization sets. Transferring geological uncertainty into SAGD production uncertainty includes (1) calculating local connectivity and connected resource assessment parameters, (2) determining potential SAGD drainage volumes, (3) extracting the geological realizations within the drainage volumes, (4) down-scaling the geological realizations within the drainage volumes, (5) rank the fine-scale geological realizations and select low, medium and high cases for flow simulation input, (6) perform flow simulation for OP_{RATE} and SOR and (7) calibrate the OP_{RATE} and SOR results to the geological ranking parameter.

This work assumes the SAGD drainage volumes that are influenced by the cumulative steam chambers of SAGD well pairs are simple rectangular prisms made out of smaller rectangular prism grid cells; however, reality is much more complex. The actual drainage volume outline will never be exactly this shape; instead, the drainage volume shape depends on time, geology and process operations. An effort to improve the estimation of the steam chamber volume of influence is warranted. For example, as experience accumulates, a library of time, geology and process dependant steam chamber training images could be developed to better guide local connectivity window dimensions and drainage volume extraction bounds.

Choosing the drainage volumes to extract and prepare for flow simulation is a key step in the SAGD reservoir characterization process. Drainage volumes that are too small will not produce the entire connected reservoir while drainage volumes that are too large would interest and complicate flow during the extraction process. Flow simulation for production performance is performed on individual drainage volumes, one at a time, which requires an assumption that the corresponding cumulative steam chambers will produce all of the connected oil in the reservoir and they will never overlap during the extraction process. Reserve forecasting is also based on an assumption of non-overlapping drainage volumes producing the entire connected reservoir. These assumptions could be poor with incomplete geological and process knowledge. The drainage volumes must be chosen in a way that best represents the cumulative steam chamber volumes of influence.

The flow of steam and oil immediately surrounding the production and injection well is critical knowledge for characterizing SAGD behavior. A localized grid refinement around SAGD well pairs may significantly improve site-specific understanding of the SAGD process. A combination of a high resolution radial grid around the well pairs with a regular Cartesian grid for the remaining reservoir volume could be used. Direct Sequential Simulation (DSS) is a well developed and proven technology available to simulate structural, lithology and petrophysical geological parameters onto non-Cartesian grids.

SAGD requires a special implementation of flow simulation in that a fine scale geological model is needed to accurately model the interaction between the steam chamber and oil within drainage volumes. The down-scaling procedure creates a number of scaling possibilities and issues. The re-simulation procedure used in this work, for example, involves re-scaling all of the variogram models to the drainage volume area. The down-scaling procedure should be chosen and implemented based on required detail and resources available.

Flow simulation input must be reduced to avoid the computer resources demand associated to inputting all drainage volume realizations at all drainage volume locations in the reservoir. Several geological ranking parameters can be used to select drainage volume realizations that span geological uncertainty. In this work, connected drainage volume was used. Another ranking system could be the optimum production well position based on maximizing connected drainage volume above the well location. In addition to reducing flow simulation input, this ranking parameter would provide optimum production well positions. The optimization procedure would be constrained by the connected base surface calculated by the local connectivity program.

Conclusion

SAGD flow response is related to geological heterogeneity. OP_{RATE} and SOR production uncertainty is captured by geological uncertainty characterized by geostatistical methods.

References

- Alberta Research Council (ARC) and Alberta Energy Research Institute (AERI), 2001. *Thermal Gravity Processes*, Power-point, AERI/ARC Core Industry Research Program.
- Denbina, E.S., 1998. *SAGD Comes of AGE!*, Journal of Canadian Petroleum Technology, 37(7):9-12.
- Pooladi-Darvish, M. and Matter, L., 2001. *SAGD Operations in the Presence of Overlying Gas Cap and Water Layer – Effect of Shale Layers*, Canadian Institute of Mining and Metallurgy (CIM), no. 178.

- Card, C.C., Woo, J. S., Wang, C. and Hu, Z., 1998. *CNPC Liaohe Dual Well SAGD – The Journey from Vision to Reality*, Canadian Institute of Mining and Metallurgy (CIM), no. 134.
- Komery, D. P., Luhning, R. W. and Pearce, J. V., 1998. *Pilot Testing of Post-Steam Bitumen Recovery from Mature SAGD Wells in Canada*, Canadian Institute of Mining and Metallurgy (CIM), no. 214.
- Shangqi, L., Yongrong, G., Zhimian, H., Naiqun, Y., Liping, Z. and Suning, H., 1998. *Study on Steam Assisted Gravity Drainage with Horizontal Wells for Super-Heavy Crude Reservoir*, Canadian Institute of Mining and Metallurgy (CIM), no. 217.
- Komery, D.P., Luhning, R.W. and O'Rourke, J.C., 1999. *Towards Commercialization of the UTF Project Using Surface Drilled Horizontal SAGD Wells*, Journal of Canadian Petroleum Technology, 38(9):36-40.
- Das, S.K., 1998. *Vapex: An Efficient Process for the Recovery of Heavy Oil and Bitumen*, Society of Petroleum Engineering (SPE), no. 50941, 3(30):232-236.
- Edmunds, N.R. and Sugget, J.C., 1995. *Design of a Commercial SAGD Heavy Oil Project*, International Heavy Oil Symposium, June 1995, Calgary, Alberta, Canada.
- Singhai, A.K, Das, S.K., Leggitt, S.M., Kasraie, M. and Ito, Y., 1996. *Screening of Reservoirs for Exploitation by Application of Steam Assisted Gravity Drainage/Vapex Processes*, International Conference on Horizontal Well Technology, November 1996, Calgary, Alberta, Canada.
- Palmgren, C. and Edmunds, N., 1995. *High Temperature Naptha to Replace Steam in the SAGD Process*, International Heavy Oil Symposium, June 1995, Calgary, Alberta, Canada.
- Edmunds, N., 1999. *SAGD: Present and Future Challenges*, APEGGA Professional Development Conference, April 1999, Calgary, Alberta, Canada.
- Llaguno, P.E., Moreno, F., Garcia, R., Mendez, Z., Escobar, E., 2002. *A Reservoir Screening Methodology for SAGD Applications*, Canadian International Petroleum Conference, June 2002, Calgary, Alberta, Canada.
- Gong, J., Polikar, M. and Chalaturnyk, R.J., 2002. *Fast SAGD Geomechanical Mechanisms*, Canadian International Petroleum Conference, June 2002, Calgary, Alberta, Canada.
- Akgun, F., 2002. *Drilling Stable Horizontal Wells – A Key Problem in Modern Oil Well Drilling*, Canadian International Petroleum Conference, June 2002, Calgary, Alberta, Canada.
- Deutsch, C. V., Dembicki, E. and Yeung, K. C., 2002. *Geostatistical Determination of Production Uncertainty: Application to Firebag Project*, Center for Computational Geostatistics (CCG), University of Alberta, Edmonton, Alberta, Canada.
- Norrena, K. P., Deutsch, C. V., 2002. *Automatic Determination of Well Placement Subject to Geostatistical and Economical Constraints*, SPE International Thermal Operations and Heavy Oil Symposium and International Horizontal Well Technology Conference, November 2002, Calgary, Alberta, Canada.

Figures

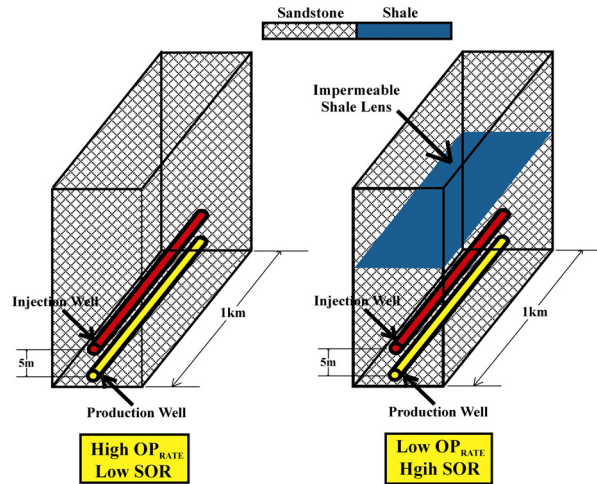


Figure 1 – Geology Affects SAGD Production. A SAGD well pair within sand (left) will have a higher OP_{RATE} and lower SOR relative to an identical well pair located below an impermeable shale facies (right).

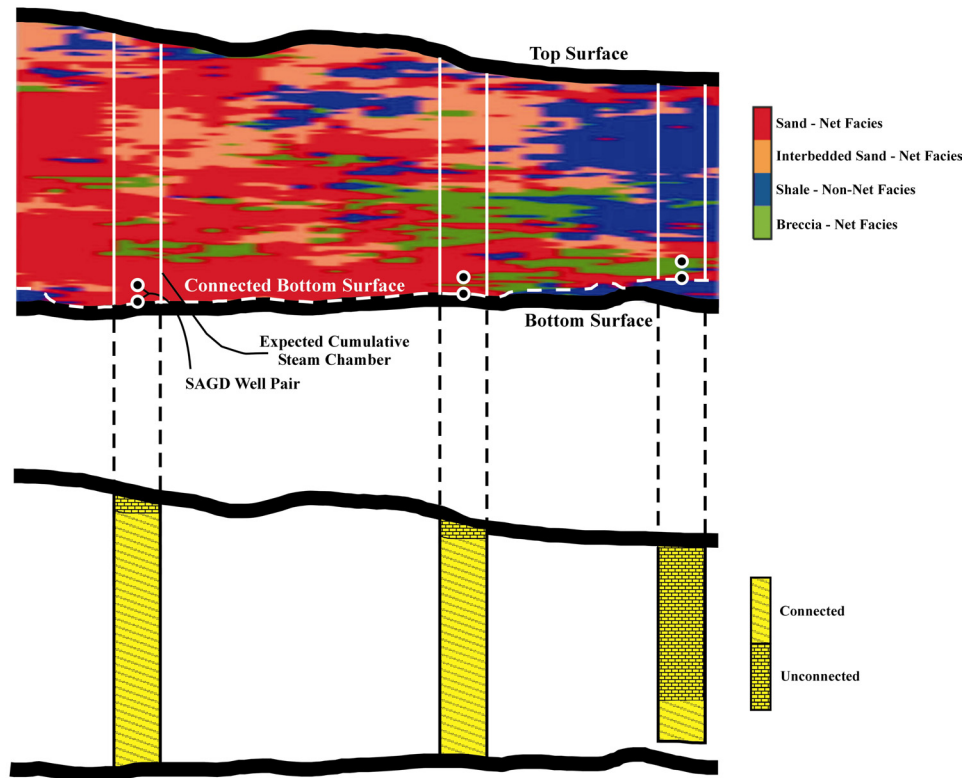


Figure 2 – Local Connectivity. A cross section through a net/non-net lithology model and the expected drainage volumes of three SAGD well pairs (white) are shown. The production wells are coincident with the connected bottom surface elevations (broken white line). For the left and middle drainage volume columns, shale ineffectively impedes the cumulative steam chamber within the drainage volume and renders most of the column connected. However, for the right drainage volume column, a low elevation shale lens effectively impedes the steam chamber rendering most the column unconnected.

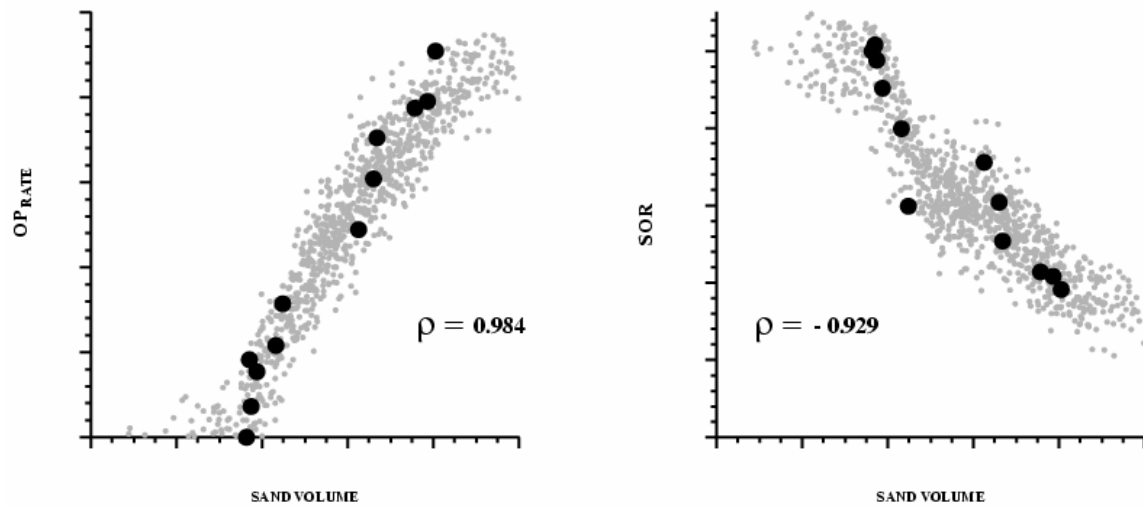


Figure 3 – Calibration of Flow Simulation Results. The cross plots show OP_{RATE} (left) and SOR (right) versus sand volume. The large black dots represent the OP_{RATE} and SOR flow response of the p10, p50 and p90 sand volume realizations within four potential SAGD drainage volumes in the reservoir. The smaller grey dots are synthetic performance output created to fit the linear correlation trend defined by the 12 flow simulation runs. The expected OP_{RATE} and SOR flow responses for any potential SAGD drainage volume in the reservoir is available through this calibration.

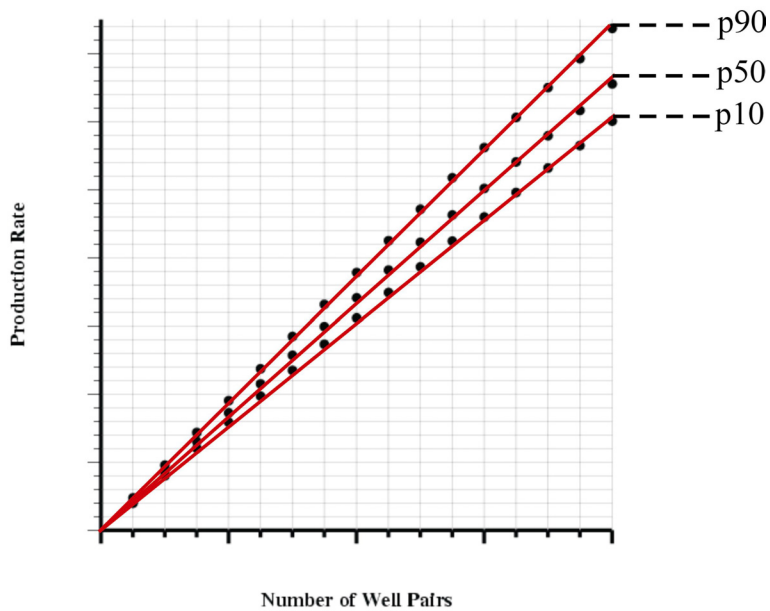


Figure 4 – Using SAGD Production Uncertainty for Decision Making. A plot of the p10, p50 and p90 OP_{RATE} versus the number of SAGD well pairs in the reservoir is shown. The number of well pairs needed to achieve a specified production target is available in this plot.

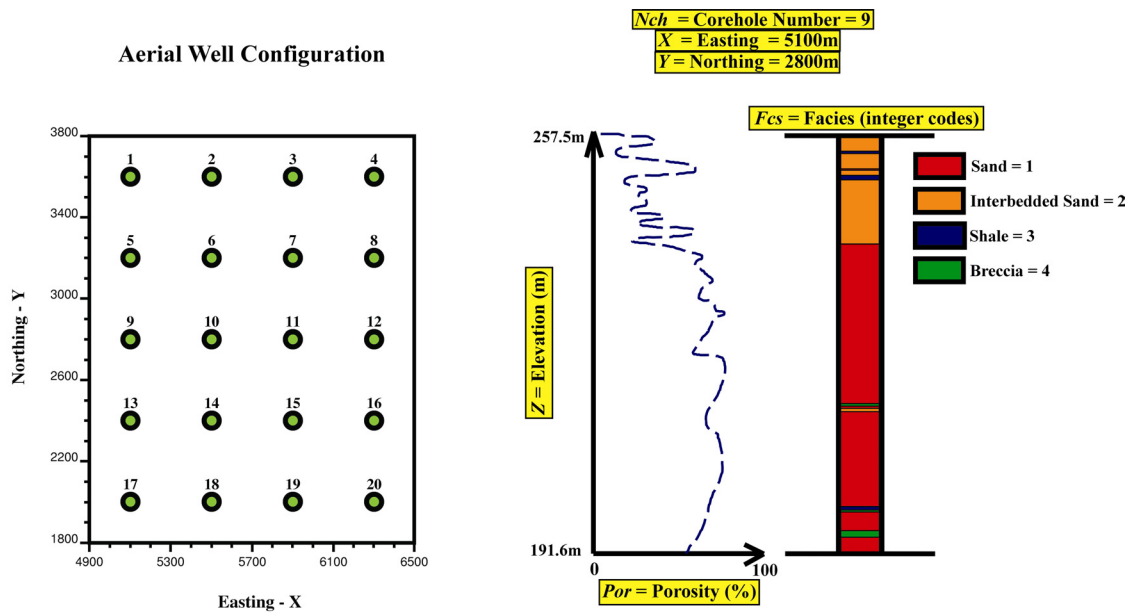


Figure 5 – Corehole Data. A plan view of the exploration corehole locations within the study area is shown on the left. For each corehole, six variables are considered. These variables and their values for corehole 9 are illustrated on the right.

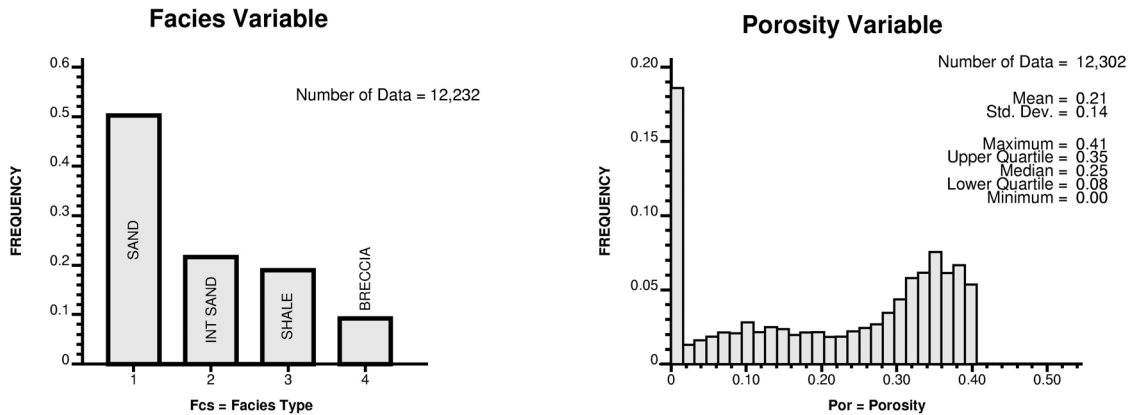


Figure 6 – Facies and Porosity Distributions. A histogram of the facies (left) and porosity (right) variable. The tri-modal shape of the porosity distribution indicates the control that the facies variable has on porosity.

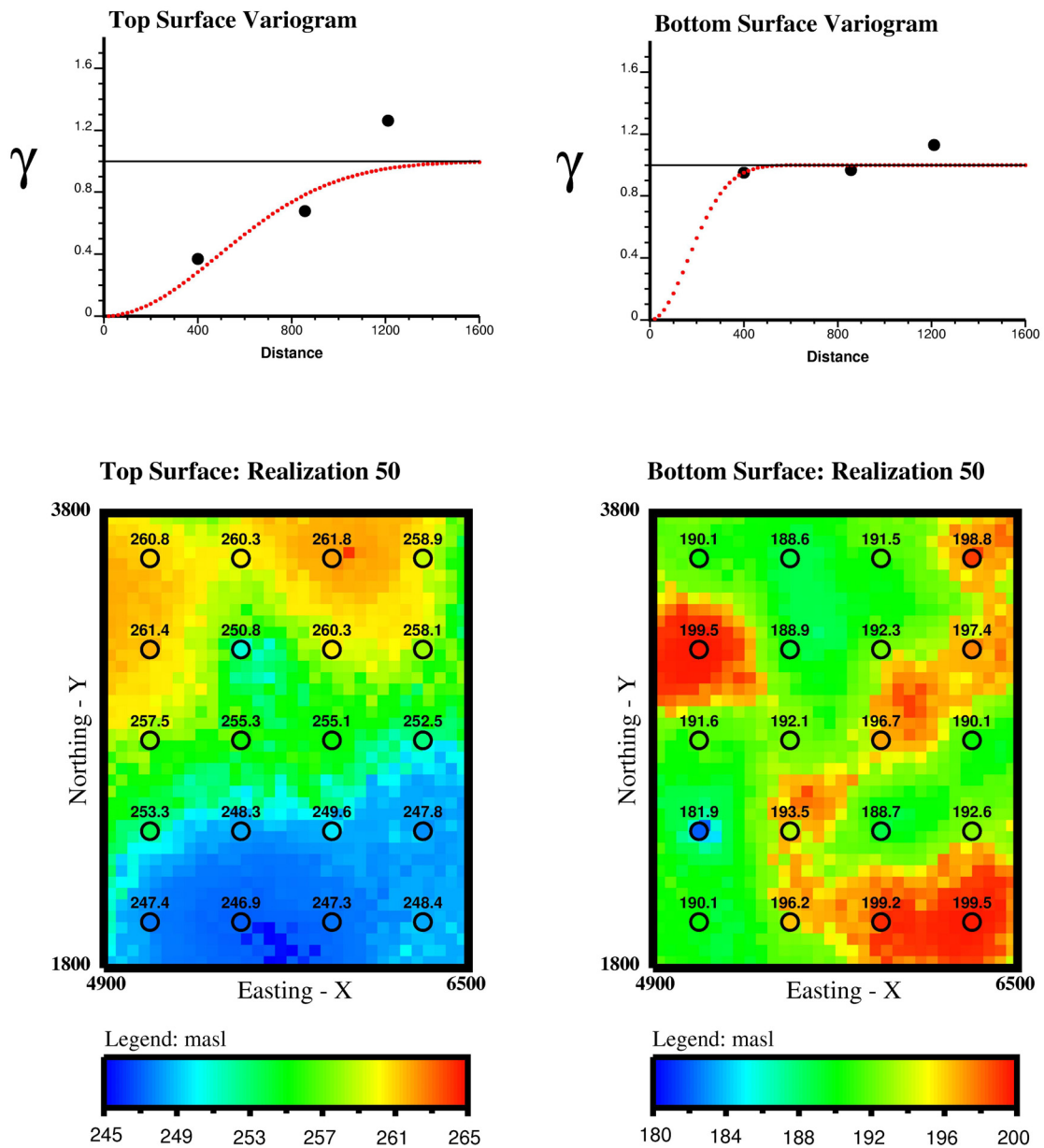


Figure 7 – Structure Modeling. The top and bottom surface variograms are shown at the top of the figure. The experimental points are represented with black dots and the variogram models are shown as broken lines. The 50th top and bottom surface realizations superimposed on their corresponding conditioning data are shown at the bottom of the figure. The units are meters above sea level (masl).

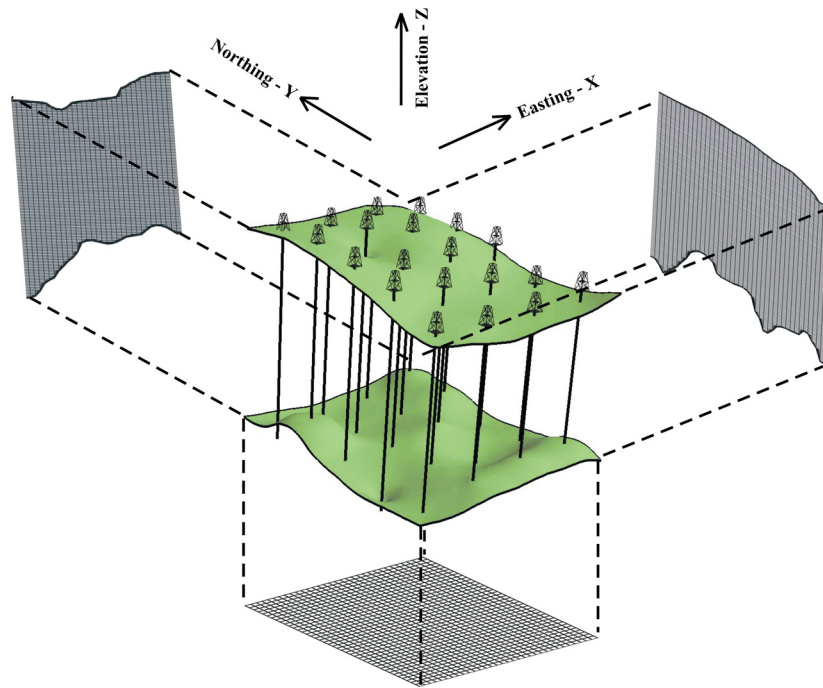


Figure 8 – Gridding. The average top and bottom surfaces are shown with the 20 corehole traces. A central easting, northing and elevation cross-section through the grid system is also shown. The easting and northing grid cross sections are clipped by the mean top and bottom surfaces shown.

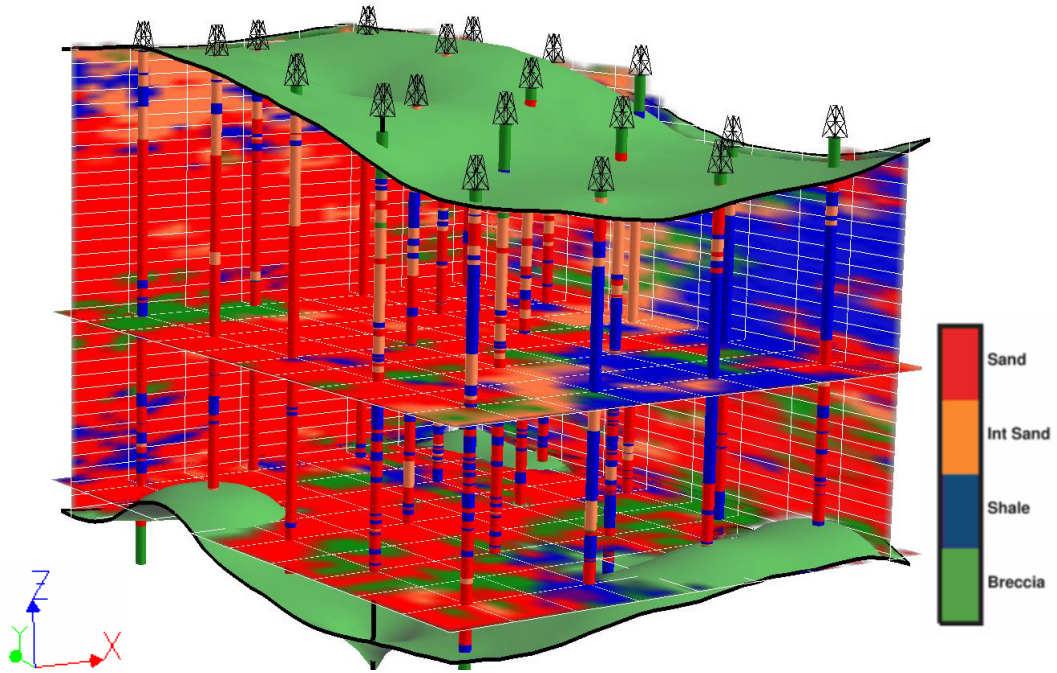


Figure 9 – Facies Simulation. An easting, northing and two elevation cross sections through the 50th facies realization. The raw facies data are also shown along the corehole traces.

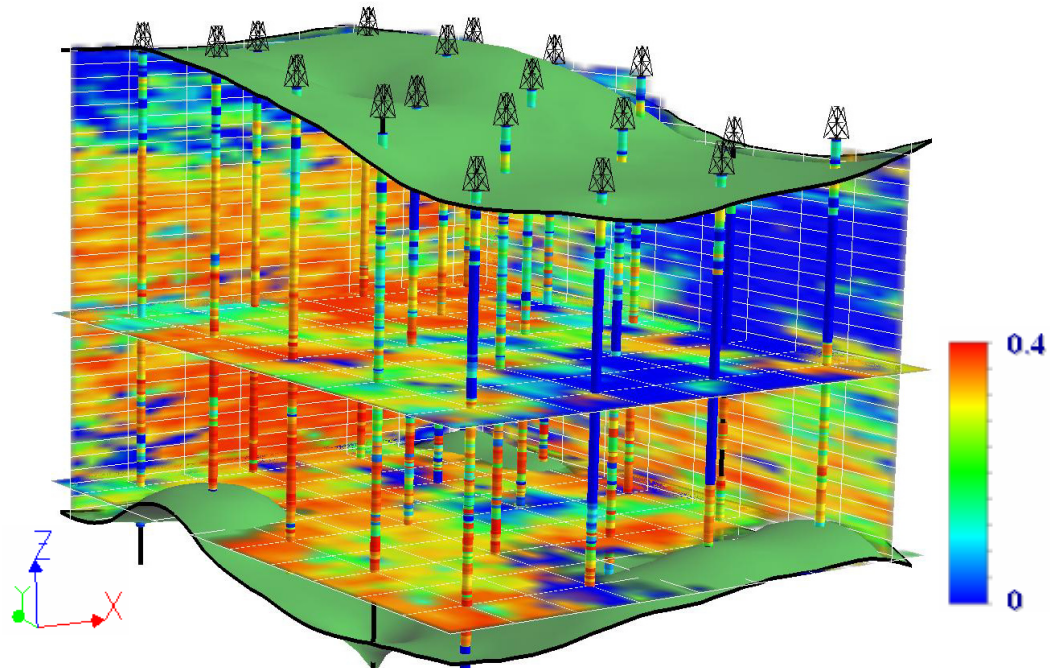


Figure 10 – Porosity Simulation. An easting, northing and two elevation cross sections through the 50th porosity realization. The raw porosity data are also shown along the corehole traces. The porosity units are in %.

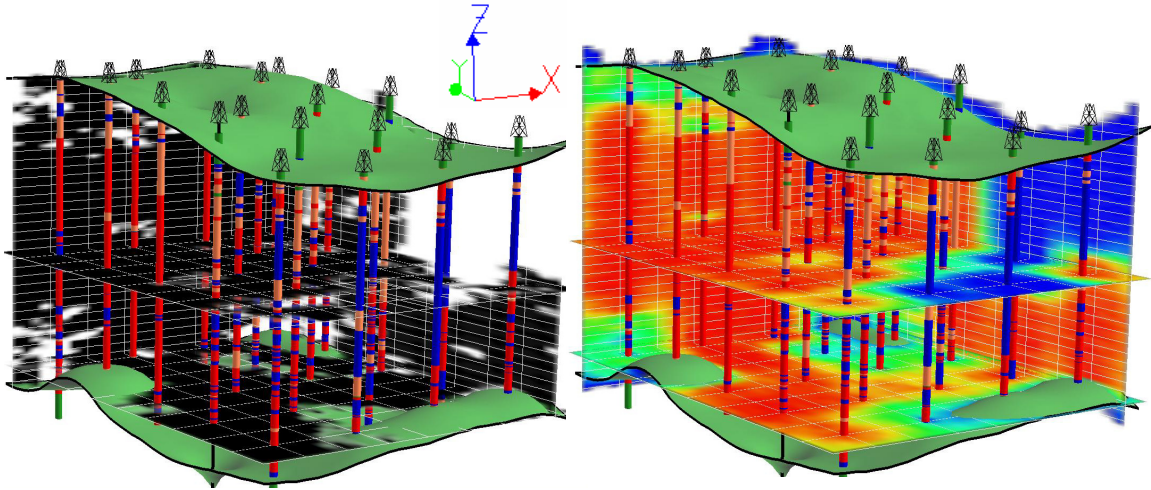


Figure 11 – Connectivity Calculation. An easting, northing and two elevation cross sections through the 50th connectivity realization is shown on the left. Connected cells are black and unconnected cells are white. The probability of connection is shown on the right. The cold-hot scale ranges from 0.0 probability (blue) to 1.0 probability (red).

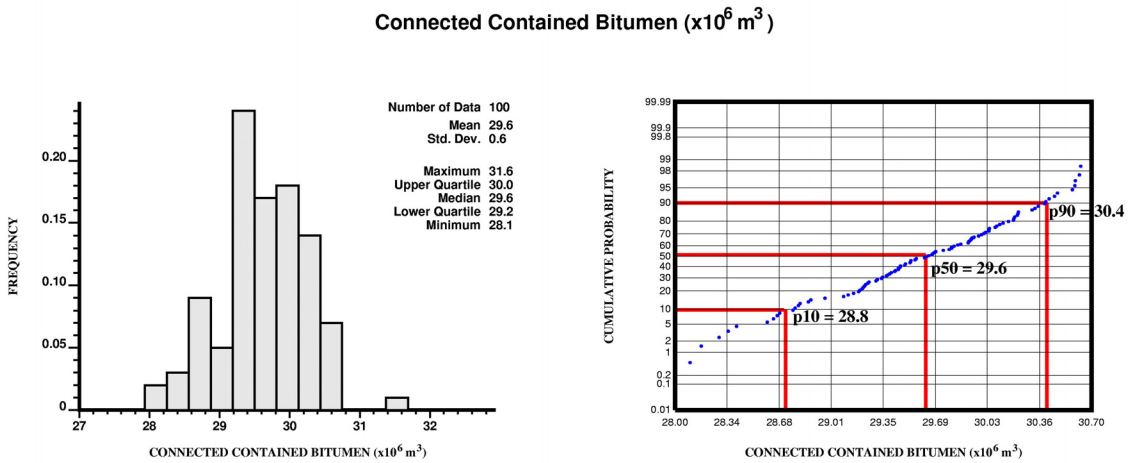


Figure 12 – Connected Contained Bitumen. A histogram and probability plot of the connected contained bitumen calculated using the geological realizations and the connectivity model.

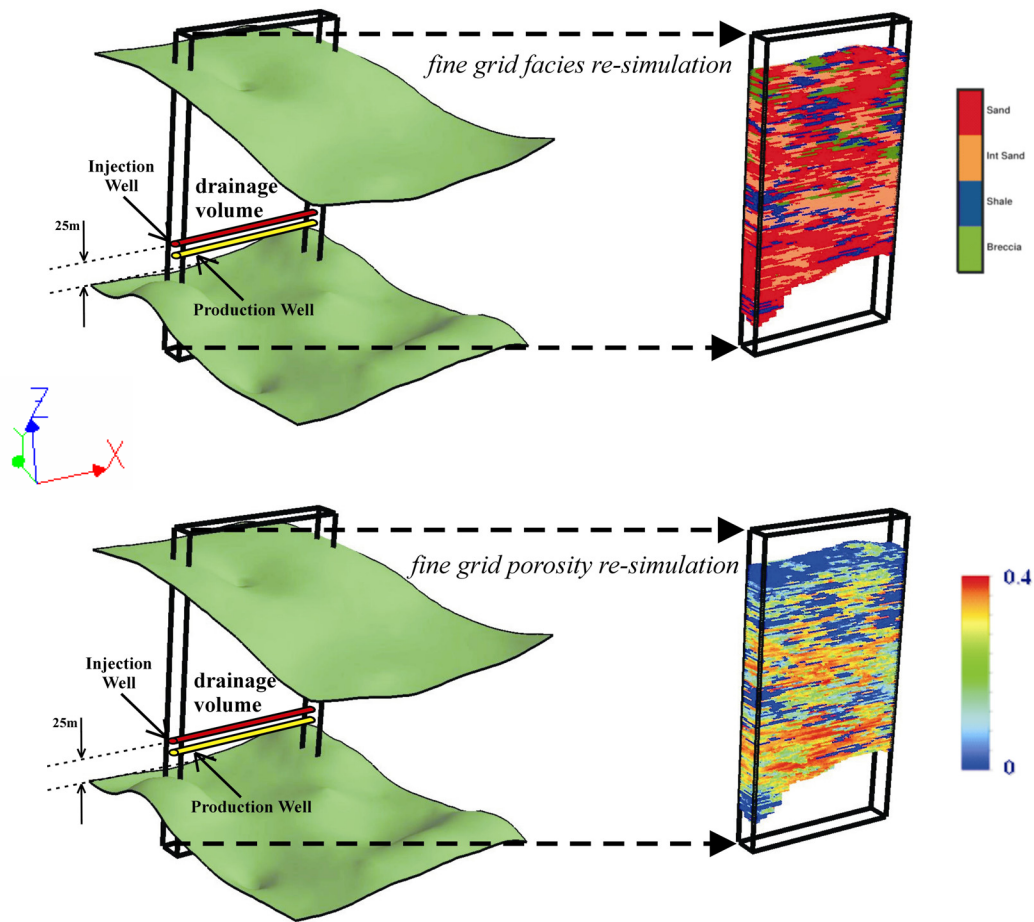


Figure 13 – Extraction and Re-gridding. An illustration of the volume extracted from the reservoir (left) and prepared for flow simulation. The 50th down-scaled facies and porosity realization are also shown (right) within the drainage volume.

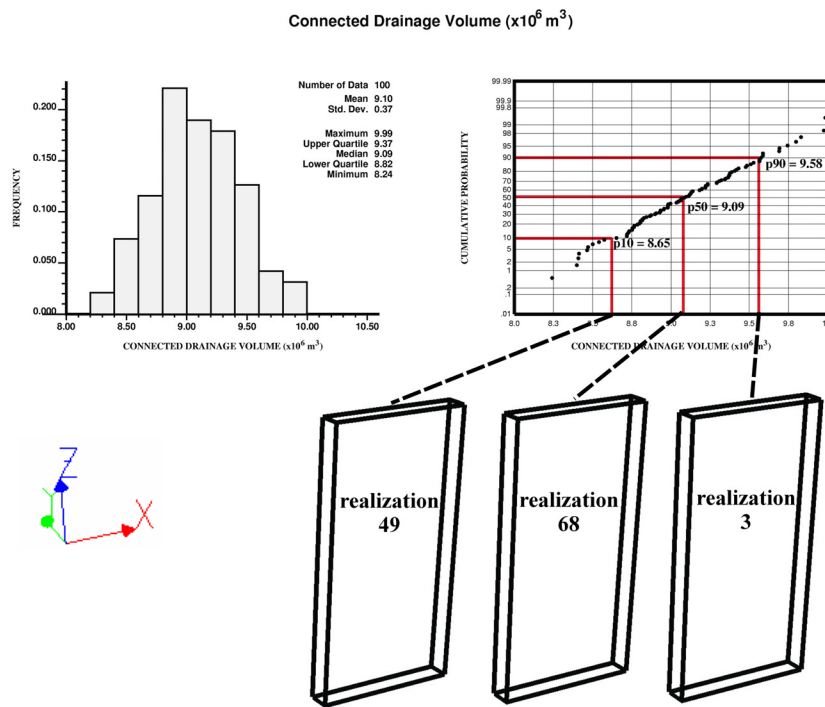


Figure 14 – Ranking. A histogram and probability plot of the connected drainage volume calculated from the fine-scale geological drainage volume realizations are shown. Realization 49, 68 and 3 are appropriate input into flow simulation for SAGD production performance appraisal.